Carbohydrate Polymers 96 (2013) 586–592

Contents lists available at SciVerse ScienceDirect

Carbohydrate Polymers

journal homepage: www.elsevier.com/locate/carbpol

Eugenol-loaded chitosan nanoparticles: II. Application in bio-based plastics for active packaging

Sarekha Woranuch[a,b], Rangrong Yoksan[a,b,*]

[a] Department of Packaging and Materials Technology, Faculty of Agro-Industry, Kasetsart University, Bangkok 10900, Thailand
[b] Center for Advanced Studies in Nanotechnology and its Applications in Chemical, Food and Agricultural Industries, Kasetsart University, Bangkok 10900, Thailand

ARTICLE INFO

Article history:
Received 21 May 2012
Received in revised form
12 September 2012
Accepted 13 September 2012
Available online 11 October 2012

Keywords:
Active packaging
Antioxidant
Chitosan nanoparticle
Eugenol
Thermoplastic flour

ABSTRACT

The aim of the present research was to study the possibility of using eugenol-loaded chitosan nanoparticles as antioxidants for active bio-based packaging material. Eugenol-loaded chitosan nanoparticles were incorporated into thermoplastic flour (TPF) – a model bio-based plastic – through an extrusion process at temperatures above 150 °C. The influences of eugenol-loaded chitosan nanoparticles on crystallinity, morphology, thermal properties, radical scavenging activity, reducing power, tensile properties and barrier properties of TPF were investigated. Although the incorporation of 3% (w/w) of eugenol-loaded chitosan nanoparticles significantly reduced the extensibility and the oxygen barrier property of TPF, it provided antioxidant activity and improved the water vapor barrier property. In addition, TPF containing eugenol-loaded chitosan nanoparticles exhibited superior radical scavenging activity and stronger reducing power compared with TPF containing naked eugenol. The results suggest the applicability of TPF containing eugenol-loaded chitosan nanoparticles as an antioxidant active packaging material.

1. Introduction

Recently, active packaging received much attention due to its ability to maintain product quality and safety, and to prolong shelf life. The demand for active packaging systems, comprised of a low-environmental-impact polymer matrix and natural antimicrobial/antioxidant agents, is growing significantly.

Thermoplastic starch/flour (TPS/TPF) have great potential as bio-based packaging materials derived from biological raw materials (e.g. corn, potato, rice and wheat) which are renewable, non-toxic, cheap and biodegradable. Only a few current works have described starch-based active packaging prepared through extrusion technology. Nam, Scanlon, Han, and Izydorczyk (2007) reported that lysozyme-embedded extruded pea starch exhibited effective antimicrobial activity against *Brochothrix thermosphacta*. However, lysozyme recovery into the active film decreased with increasing extrusion temperature. Another related work studied the incorporation of oregano essential oil into cassava starch–chitosan films to obtain antimicrobial active materials against *Bacillus cereus*, *Escherichia coli*, *Salmonella enteritidis* and *Staphylococcus aureus* (Pelissari, Grossmann, Yamashita, & Pineda, 2009).

Eugenol, a natural phenolic compound primarily extracted from clove plants, has been widely used in foods, pharmaceuticals, cosmetics, and active packaging materials (Sanla-Ead, Jangchud, Chonhenchob, & Suppakul, 2012) due to its potent antimicrobial and antioxidant properties (Baskaran, Periyasamy, & Venkatraman, 2010; Devi, Nisha, Sakthivel, & Pandian, 2010). However, most plant-derived phenolic compounds are sensitive to oxygen, light and heat (Chalier, Ben Arfa, Preziosi-Belloy, & Gontard, 2007; Choi, Soottitantawat, Nuchuchua, Min, & Ruktanonchai, 2009; Coimbra et al., 2011). Previously, we found that encapsulation of eugenol into chitosan-TPP nanoparticles could reduce the loss of eugenol during exposure to a severe environment, i.e. heat (Woranuch & Yoksan, 2012). Many research groups have investigated the utilization of encapsulated plant-derived phenolic compounds in food, cosmetic and pharmaceutical applications (Munin & Edwards-Lévy, 2011; Nonsee, Supitchaya, & Thawien, 2011); however, none of these reports have focused on the area of active packaging.

Although the greater antioxidant activity of TPF containing eugenol-loaded chitosan-TPP nanoparticles compared with TPF containing naked eugenol was preliminarily studied in our previous work (Woranuch & Yoksan, 2012), the effect of eugenol-loaded chitosan-TPP nanoparticles on other properties of TPF related to packaging applications was not addressed. In many cases, chitosan-TPP nanoparticles have been incorporated into polymer matrices such as starch (Chang, Jian, Yu, & Ma, 2010) and hydroxypropyl methylcellulose (Jayakumar et al., 2010) through a solvent casting process to improve certain characteristics of the polymer films. Advanced bio-based plastic conversion technologies, such as

* Corresponding author at: Department of Packaging and Materials Technology, Faculty of Agro-Industry, Kasetsart University, Bangkok 10900, Thailand. Tel.: +66 2 562 5097; fax: +66 2 562 5046.
E-mail addresses: rangrong.y@ku.ac.th, yyrangrong@yahoo.com (R. Yoksan).

0144-8617/$ – see front matter © 2012 Elsevier Ltd. All rights reserved.
http://dx.doi.org/10.1016/j.carbpol.2012.09.099

extrusion, film blowing and injection molding, are still required to meet industrial-scale production of active bio-based packaging materials.

Therefore, the objective of the present research was to prepare active bio-based packaging material based on TPF and eugenol-loaded chitosan-TPP nanoparticles by an extrusion process. The influences of eugenol-loaded chitosan nanoparticles on crystallinity, morphology, thermal properties, radical scavenging activity, tensile properties, and water vapor and oxygen barrier properties of TPF were also investigated.

2. Materials and methods

2.1. Materials

Chitosan (degree of deacetylation of 0.95 and molecular weight of ~700 kDa) was purchased from Seafresh Chitosan (Lab), Thailand. Eugenol (99%) and 2,2-diphenyl-1-picrylhydrazyl (DPPH) were acquired from Sigma–Aldrich, Germany. Pentasodium tripolyphosphate (TPP) and Tween 60 were supplied by Fluka Chemika, Switzerland. Acetic acid, hydrochloric acid and ethanol (95%) were purchased from Merck, Germany. Potassium ferricyanide was purchased from Ajax Finechem, Australia. Trichloroacetic acid was acquired from Fisher Scientific, United Kingdom. Ferric chloride was obtained from Loba Chemie, India. Cassava starch was supplied by Tong Chan, Thailand. Rice flour and waxy rice flour were products of Cho Heng Rice Vermicelli Factory, Thailand. The glycerol used was of commercial grade.

2.2. Preparation of eugenol-loaded chitosan nanoparticles

Eugenol-loaded chitosan nanoparticles were prepared by a method comprising oil-in-water emulsion and ionic gelation, according to our previous report (Woranuch & Yoksan, 2012). A weight ratio of chitosan to eugenol of 1:1 and a concentration of pentasodium tripolyphosphate of 0.5% (w/w) were used in the present study.

2.3. Preparation of thermoplastic flour containing eugenol-loaded chitosan nanoparticles

Seven formulations of thermoplastic flour (TPF) were prepared using different compositions, as shown in Table 1. Mixed flour (cassava, rice and waxy rice flours in a weight ratio of 50:30:20), glycerol (30%, w/w) and other additional additives (Table 1) were blended in a mixer (model 20L; Mitsubishi, Japan). The mixture was then blended in a twin-screw extruder (LTE-20-40; Labtech Engineering, Thailand) using a barrel temperature ranging from 95 °C to 155 °C, a material feed rate of 25–30 rpm and a screw speed of 100–130 rpm. The extrudates were cut into 3-mm-long pellets by a pelletizer (LZ-120; Labtech Engineering). The obtained TPF pellets were dried in a hot-air oven at 45 °C for 12 h, and subsequently extruded into sheets by a twin-screw extruder attached to a flat die. Sheet extrusion was carried out at a temperature range of 70–170 °C using a material feed rate of 20–25 rpm, screw speed of 140–150 rpm and chill roll speed of 0.6 rpm. The thickness of sheets was measured at five positions on the perimeter and at the center of the sheet by a digital caliper (Mitutoyo Absolute, model ID-C 112BS, Japan) to obtain an average value.

2.4. Characterization of thermoplastic flour containing eugenol-loaded chitosan nanoparticles

X-ray diffraction (XRD) patterns were recorded by a JDX-3530 X-ray diffractometer (JEOL, Japan) over a 2θ range from 3° to 40° using a scan rate of 0.04° min^{-1}. Thermogravimetric analysis (TGA) was performed using a TGA/DSC 1 STARe (Mettler-Toledo, Switzerland) under nitrogen atmosphere with a flow rate of 50 mL min^{-1}. Each sample (7 mg) was placed in a crucible and then heated from 30 °C to 600 °C at a heating rate of 10 °C min^{-1}. Differential scanning calorimetry (DSC) analysis was performed with a Mettler-Toledo DSC 822e. Samples (7 mg each) were then packed in a DSC aluminum pan with a closed lid having a 1-mm-diameter hole at the center. The first heating scan was carried out from −50 °C to 250 °C at a heating rate of 20 °C min^{-1}. The sample was then cooled to −50 °C at a cooling rate of 20 °C min^{-1}, held at −50 °C for 5 min, and reheated from −50 °C to 250 °C at a heating rate of 20 °C min^{-1}. A nitrogen flow rate of 50 mL min^{-1} was preserved throughout the experiment.

2.5. Determination of remaining content of eugenol in thermoplastic flour

Individual samples (10 mg) were mixed with hydrochloric acid solution (2 M, 5 mL) and then boiled at 95 °C for 30 min. After cooling to room temperature, the homogeneous solution was mixed with ethanol (1 mL) by vortexing, and then centrifuged at 9000 rpm 25 °C for a few min. The supernatant was analyzed by UV–Vis spectroscopy over a wavelength ranging from 250 nm to 350 nm. The remaining content of eugenol was calculated from Eq. (1):

$$A = 24.86C \quad (R^2 = 0.9949) \tag{1}$$

where A is the absorbance at 283.5 nm of the supernatant in a sample tube, and C is the remaining content of eugenol in the sample (mg/g). TPF without incorporation of any other additional additives (TPFN) and TPF containing chitosan nanoparticles (TPFC) were used as blanks for the analysis of TPF containing free eugenol (TPFE) and TPF containing eugenol-loaded chitosan nanoparticles (TPFCE), respectively.

2.6. Evaluation of radical scavenging activity of thermoplastic flour

Radical scavenging activity of TPF was determined by a DPPH method modified from the one reported by Parejo et al. (2002). Briefly, each sample (10 mg) was immersed in an ethanolic solution of stable DPPH radical (100 μM, 100 μL) and then incubated in the dark at room temperature. TPFN and TPFC were used as controls for the analysis of TPFE and TPFCE, respectively. The absorbance

Table 1
Composition of TPF.

Sample code	Additional additive	Nanoparticle content (%, w/w)	Eugenol content (%, w/w)
TPFN	–	–	–
TPFE1	Free eugenol	–	0.35
TPFE2	Free eugenol	–	0.7
TPFCE1	Eugenol-loaded chitosan nanoparticles	3	0.35
TPFCE2	Eugenol-loaded chitosan nanoparticles	6	0.7
TPFC1	Chitosan nanoparticles	3	–
TPFC2	Chitosan nanoparticles	6	–

of the DPPH solution was measured at 517 nm. Radical scavenging activity was defined as a decrease in the absorbance of the sample versus a DPPH standard solution, and was calculated from Eq. (2):

$$\%\ \text{DPPH decoloration} = \left[\frac{\text{Abs}_{\text{control}} - \text{Abs}_{\text{sample}}}{\text{Abs}_{\text{control}}}\right] \times 100 \quad (2)$$

where $\text{Abs}_{\text{control}}$ is the absorbance of the supernatant in a control tube and $\text{Abs}_{\text{sample}}$ is the absorbance of the supernatant in a sample tube.

2.7. Evaluation of antioxidant activity of thermoplastic flour by reducing power assay

The reducing power of TPF was determined according to the method of Oyaizu (1986). Briefly, sample (10 mg) was added to a mixture of phosphate buffer (2.5 mL) and potassium ferricyanide (1%, w/v, 2.5 mL) and then heated to 50 °C for 20 min. After cooling to ambient temperature, the mixture was mixed with trichloroacetic acid (10%, 2.5 mL) and centrifuged at 9000 rpm for 10 min. The supernatant (2.5 mL) was then mixed with distilled water (2.5 mL) and a freshly prepared ferric chloride solution (0.1%, w/v, 0.5 mL). The absorbance at 700 nm of the mixture was recorded after reaction for 10 min.

2.8. Tensile testing of thermoplastic flour

TPF sheets were cut into rectangular shapes (15 cm × 2.5 cm) and conditioned in a closed chamber containing saturated sodium nitrite solution at 25 °C (65% RH) for 3 days prior to testing. Tensile properties of the samples were examined according to ASTM D882 using a Hounsfield H50KS testing machine (UK) with a load cell of 500 kN. The test was performed with a crosshead speed of 50 mm/min and a grip separation of 100 mm. Five replicates were tested for each sample to obtain an average value.

2.9. Determination of water vapor permeability of thermoplastic flour

The water vapor transmission rate (WVTR) was determined according to ASTM E398-03 using a Permatran-W model 398 (Mocon, USA). The sample sheets were cut into square shapes (7 cm × 7 cm) and sandwiched between two thin sheets of doughnut-shaped aluminum foil, leaving a test area of 5 cm^2. Testing was performed at 90% RH and 25 °C using a nitrogen flow rate of 800 cm^3/min. Water vapor permeability (WVP) was evaluated by normalization of the WVTR with respect to the water vapor pressure and sample thickness. Three replicates were tested for each sample.

2.10. Determination of oxygen permeability of thermoplastic flour

The oxygen transmission rate (OTR) was measured according to ASTM D3985 using an oxygen permeation analyzer (model 8501; Illinois Instruments, USA). The sample sheets were cut into square shapes (7 cm × 7 cm) and sandwiched between two thin sheets of doughnut-shaped aluminum foil so that an area of 28.26 cm^2 was exposed for measurement. The assembled sheets were then kept in a closed chamber containing saturated calcium chloride solution at 25 °C (50% RH) for at least 48 h prior to measurement. Testing was performed at 0% RH and ambient temperature. Oxygen permeability (OP) was evaluated by normalization of the OTR with respect to the oxygen pressure and sample thickness. Three replicates were tested for each sample.

3. Results and discussion

TPF containing eugenol-loaded chitosan nanoparticles (TPFCE) was prepared by extrusion, which is a thermal process in which the plastic is heated and experiences shear force from pressing the molten material through a die. In the present work, extrusion was carried out twice to obtain products in the form of pellets and sheets, respectively. Preparation of TPF pellets was performed at a temperature range of 95–155 °C, while a wider temperature range of 70–170 °C was used to fabricate TPF sheets. TPF without incorporation of any other additional additives (TPFN), TPF containing free eugenol (TPFE), and TPF containing chitosan nanoparticles (TPFC) were also prepared (Table 1) and used as controls or in some cases used for comparison with TPFCE.

The packing structure of TPF was analyzed by XRD technique. TPFN exhibited diffraction peaks at 2θ of 13° and 20°, corresponding to a V-type crystal structure (Ma, Yu, & Wan, 2006; Yokesahachart & Yoksan, 2011). The V-type conformation might involve the formation of amylose–glycerol complexes (Ma et al., 2006). The incorporation of eugenol, chitosan nanoparticles and eugenol-loaded chitosan nanoparticles, with a content of no more than 0.7% (w/w), 6% (w/w) and 6% (w/w), respectively, did not affect the crystal type of TPF.

Thermal properties of TPF were analyzed by TGA and DSC techniques. TGA is a useful technique to investigate the mass loss of a sample upon heating at a given heating rate. All TPF underwent a three-step mass loss, at temperatures below 100 °C and in the ranges of 188–200 °C and 288–337 °C; this may be attributed to the evaporation of moisture, volatilization of glycerol and decomposition of flour, respectively (Ma et al., 2006; Yokesahachart & Yoksan, 2011). It should be noted that the incorporation of eugenol did not affect the maximum mass loss temperature of TPF. In contrast, the maximum mass loss temperature of TPF tended to decrease when chitosan nanoparticles and eugenol-loaded chitosan nanoparticles were added. This reflected reduced thermal stability of TPF containing nanoparticles.

The decomposition temperature (T_d) is generally defined as the temperature corresponding to the highest mass loss rate, which is clearly observed as a peak in the DTG thermogram plotting mass loss rate and temperature. T_d of flour for all types of TPF appeared at 275–311 °C. The insignificant change of T_d of flour for TPFE might be explained by the existence of a tiny amount of eugenol in the TPF matrix (Table 2). The reduction of T_d of flour for TPFC and TPFCE (~19–35 °C) compared with that of TPFN might possibly be due to the suppressed retrogradation or restrained recrystallization of starch molecules by the impedance of nanoparticle agglomerates. However, Jayakumar et al. (2010) found that T_d of hydroxypropyl methylcellulose increased by adding chitosan-TPP nanoparticles due to strong H-bond formation between hydroxypropyl methylcellulose and the nanoparticles. It should be pointed

Table 2
Remaining content of eugenol in TPF pellets and sheets.

Form of sample	Sample	Remaining content of eugenol* (mg/g)
Pellet	TPFE1	0.002 ± 0.0003^{e}
	TPFE2	0.033 ± 0.0006^{d}
	TPFCE1	0.076 ± 0.001^{b}
	TPFCE2	0.303 ± 0.006^{a}
Sheet	TPFE1	n.d.
	TPFE2	n.d.
	TPFCE1	0.036 ± 0.005^{d}
	TPFCE2	0.055 ± 0.005^{c}

n.d., not detected.

* Each value represents the mean ± SD ($n = 3$). Different superscript letters in the same column show a significant difference ($p < 0.05$) by Duncan's multiple range test.

out that the nature of the polymer matrix, particle agglomeration and the conversion process might affect H-bond formation and recrystallization of the continuous phase.

DSC is a thermoanalytical technique used to study the thermal transitions of a polymer. Data from the first heating scan showed that TPFN exhibited an endothermic peak at 196 °C, corresponding to the melting temperature (T_m) of TPF. T_m of TPFE, TPFC and TPFCE appeared in a range from 196 °C to 211 °C. However, the observed T_m of one sample could not be exactly compared with the others due to its different thermal history. It should be pointed out that the applied cooling rate of 20 °C min^{-1} was too fast to allow large molecules of starch to crystallize; as a result there was no information obtained from the cooling scan, and no T_m was observed in the second heating scan (data not shown). When considering the enthalpy of melting, it was found that ΔH_m of TPFN was 95.3 J/g. Incorporation of eugenol, chitosan nanoparticles and eugenol-loaded chitosan nanoparticles reduced ΔH_m of TPF to values ranging from 67.4 J/g to 88.7 J/g, implying that starch crystals were more easily destroyed. The reduction of ΔH_m for TPFE might be explained by the plasticization effect of eugenol. On the other hand, the reason for decreased ΔH_m of TPFC and TPFCE might relate to the restrained retrogradation/recrystallization of starch molecules by nanoparticles.

The content of eugenol remaining in TPF after extrusion was determined by UV–Vis spectroscopy at a λ_{max} of 283.5 nm. The remaining contents of eugenol in TPFE1 and TPFE2 pellets were 0.002 mg/g and 0.033 mg/g, respectively, while those of TPFCE1 and TPFCE2 pellets were 0.076 mg/g and 0.303 mg/g, respectively (Table 2). The results showed that the remaining eugenol content in TPF increased with higher initial content of eugenol. In addition, TPFCE possessed a higher remaining content of eugenol than TPFE, implying that the encapsulation of eugenol into chitosan nanoparticles could reduce the loss of eugenol during thermal processing. TPFE sheets did not exhibit an absorption peak at a wavelength range from 250 nm to 400 nm, reflecting a lower remaining content of eugenol. In contrast, the remaining eugenol content in TPFCE1 and TPFCE2 sheets could be determined from the maximum absorption peak at 283.5 nm as 0.036 mg/g and 0.055 mg/g, respectively (Table 2). This result confirmed that the loss of eugenol during the extrusion process could be decreased by its encapsulation into the nanoparticles. Furthermore, TPF sheets had lower remaining content of eugenol than TPF pellets, suggesting that the number of thermal exposures affected the remaining content of eugenol, i.e. the amount of eugenol retained in TPF was reduced when the number of thermal exposures increased.

Antioxidant efficiency of eugenol in TPF was evaluated by a DPPH method. A freshly prepared DPPH solution is characteristically a deep purple color, with a maximum absorption at 517 nm. The antioxidants can quench DPPH free radicals and convert them into a colorless product, resulting in a reduction of absorbance at 517 nm. Fig. 1 illustrates that the radical scavenging percentage of both TPFE and TPFCE increases with time for the first 48 h and then levels off. The marked increase of radical scavenging percentage during the initial stage might be explained by the high diffusion rate of eugenol from the TPF matrix due to the concentration gradient. The radical scavenging percentages of TPFCE2 and TPFE2 pellets were 52.63% and 14.13%, respectively (Fig. 1a and b), indicating that TPF containing eugenol-loaded chitosan nanoparticles exhibited higher antioxidant activity than TPF containing naked eugenol. On the other hand, TPFCE2 and TPFE2 sheets (Fig. 1c and d) possessed lower radical scavenging percentages (31.33% and 13.46%, respectively) than their corresponding pellets (Fig. 1a and b). This result suggested that the antioxidant activity of TPF materials containing free eugenol and encapsulated eugenol decreased with an increased number of thermal exposures. It could be concluded from the above findings that encapsulation of eugenol into chitosan nanoparticles could reduce the loss of eugenol or improve its thermal stability during extrusion; as a result, the materials containing eugenol-loaded chitosan nanoparticles possessed higher remaining content of eugenol and showed better antioxidant properties than those containing naked eugenol.

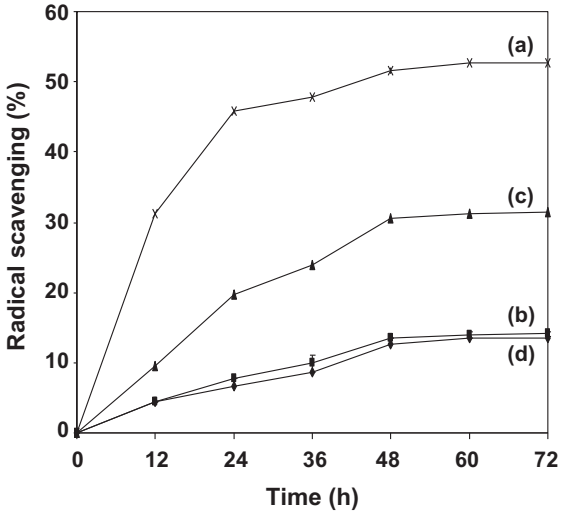

Fig. 1. Radical scavenging percentages as a function of time of different TPF pellets and sheets: (a) TPFCE2 pellet, (b) TPFE2 pellet, (c) TPFCE2 sheet and (d) TPFE2 sheet. Each point represents the mean ± SD (n = 3).

Reducing power of TPF was determined based on the chemical reaction of Fe(III) → Fe(II). The as-formed Fe(II) could react with ferric chloride to form ferric ferrous complex that has an absorption maximum at 700 nm. The higher absorbance at 700 nm indicated the stronger reducing power. TPFC2, TPFE2 and TPFCE2 pellets possessed the absorbances at 700 nm of 0.27–0.29, 0.30–0.33 and 0.58–0.90, respectively, when the reaction time was 10–50 min (Fig. 2a–c), while the absorbances at 700 nm of TPFC2, TPFE2 and TPFCE2 sheets were 0.23–0.27, 0.28–0.31 and 0.39–0.60, respectively (Fig. 2d–f). The result implied that these TPF materials could reduce Fe(III) to Fe(II). However, the reducing power of TPFCE2 was

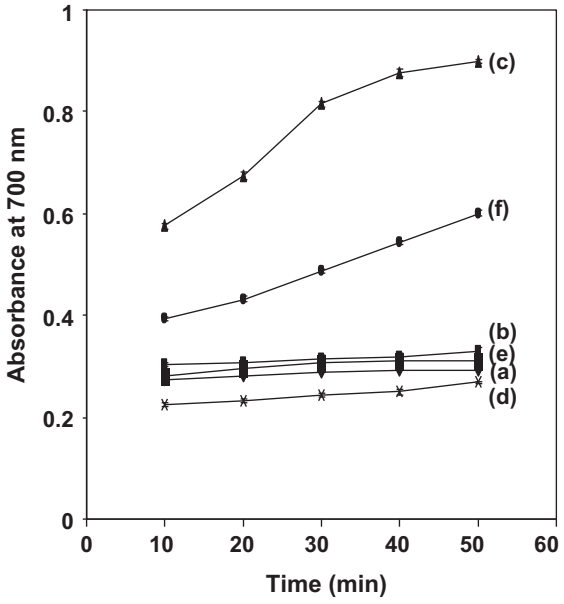

Fig. 2. Reducing power as a function of time of different TPF pellets and sheets: (a) TPFC2 pellet, (b) TPFE2 pellet, (c) TPFCE2 pellet, (d) TPFC2 sheet, (e) TPFE2 sheet and (f) TPFCE2 sheet. Each point represents the mean ± SD (n = 3).

significantly higher than those of TPFE2 and TPFC2, respectively. This might be explained by the antioxidant activity of eugenol over chitosan nanoparticles and also the reduction of eugenol loss during thermo-mechanical process of TPFCE2. In addition, TPF sheets exhibited lower reducing ability than TPF pellets indicating that increased number of thermal exposure reduced antioxidant activity of TPF material. These results supported the above finding.

Tensile strength, modulus and elongation at break of TPF sheets were determined as the stress at peak, the slope at elastic (linear) portion, and the strain at break of a stress–strain curve, respectively. TPFN showed tensile strength, modulus and elongation at break of 1.78 MPa, 51.83 MPa and 74.63%, respectively (Table 3). The incorporation of 0.35% (w/w) of eugenol caused a decrease in tensile strength, modulus and elongation at break of TPF, to values of 1.51 MPa, 34.95 MPa and 55.20%, respectively. Previously, Pelissari et al. (2009) reported that the addition of oregano essential oil to starch–chitosan films caused decreased tensile strength and Young's modulus but increased elongation at break due to the plasticizing capacity of essential oil. However, in the present study the values of tensile strength, modulus and

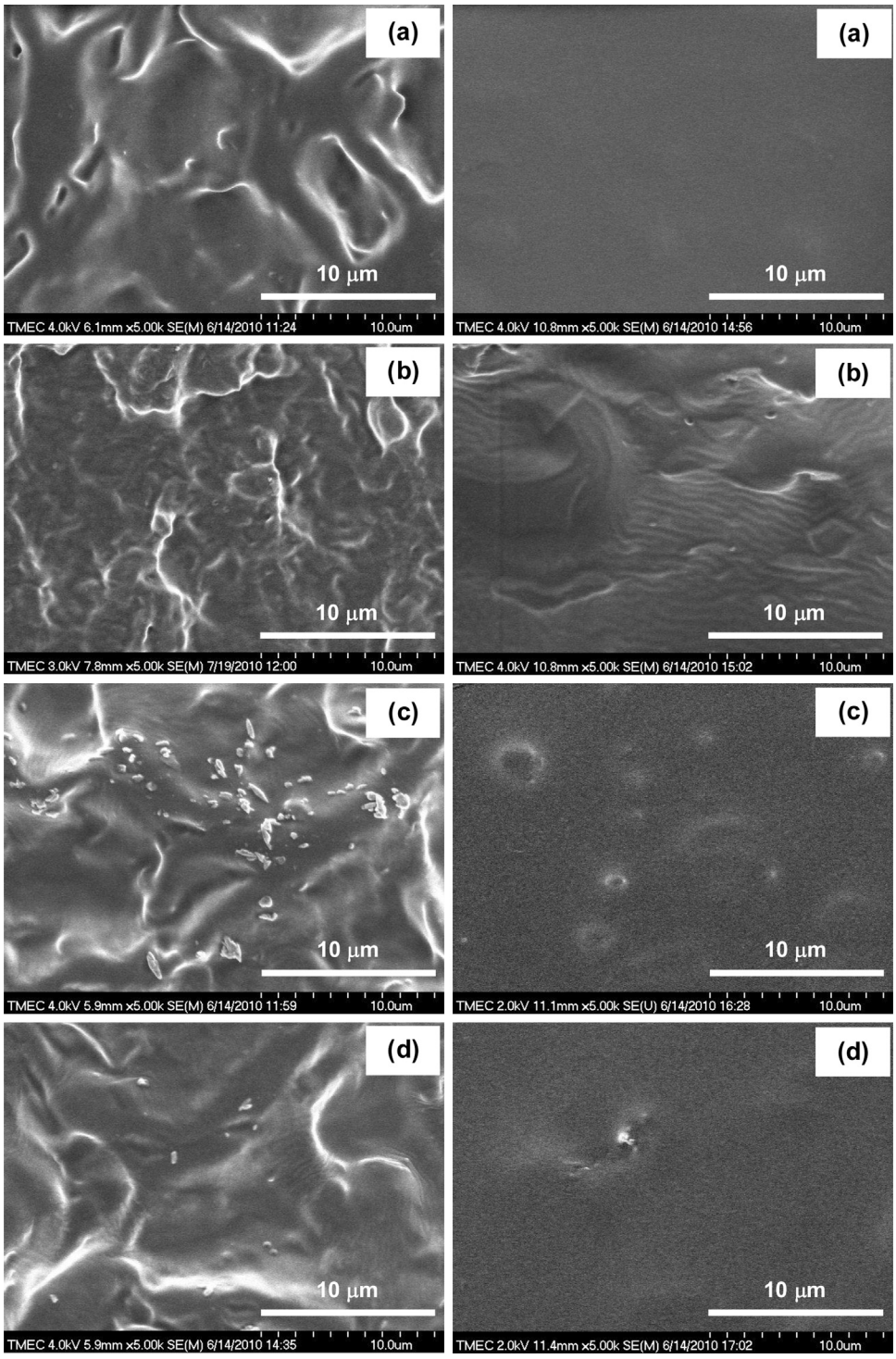

Fig. 3. SEM micrographs at 2–4 kV at sheet surface (left) and at cross section (right) of different TPF sheets: (a) TPFN, (b) TPFE1, (c) TPFC1 and (d) TPFCE1.

Table 3
Tensile properties of TPF sheets.

Sample	Tensile strength* (MPa)	Modulus* (MPa)	Elongation @ break* (%)
TPFN	1.78 ± 0.12[a]	51.83 ± 5.50[a]	74.63 ± 2.69[a]
TPFE1	1.51 ± 0.11[ab]	34.95 ± 11.03[ab]	55.20 ± 6.97[a]
TPFC1	1.22 ± 0.09[b]	21.14 ± 1.07[b]	61.33 ± 6.55[a]
TPFCE1	1.53 ± 0.23[ab]	41.03 ± 7.71[ab]	10.71 ± 2.38[b]

* Each value represents the mean ± SD ($n = 5$). Different superscript letters in the same column show a significant difference ($p < 0.05$) by Duncan's multiple range test.

elongation at break of TPFE were not significantly different from those of TPFN (Duncan's multiple range test, $p < 0.05$) because of the small amount of eugenol remaining in TPFE (Table 2). In addition, the immiscibility of hydrophilic TPF and hydrophobic eugenol (Fig. 3b, right) might be another reason for the deterioration of tensile properties. Tensile strength, modulus and elongation at break of TPF also decreased by incorporating 3% (w/w) of chitosan nanoparticles and eugenol-loaded chitosan nanoparticles: to values ranging from 1.22 MPa to 1.53 MPa, from 21.14 MPa to 41.03 MPa, and from 10.71% to 61.33%, respectively. Recently, Chang et al. (2010) disclosed that chitosan-TPP nanoparticles can reinforce glycerol plasticized starch prepared by a casting process, when a small amount of nanoparticles was loaded. However, an increased amount of chitosan nanoparticles led to particle agglomeration and consequently decreased tensile strength. In the present work, we found that chitosan nanoparticles were agglomerated in the TPFC and TPFCE matrices (Fig. 3c and d, right), which might cause poor interfacial interaction between nanoparticles and the matrix as well as induce structural fragility of the sheets. Compared with TPFC, TPFCE showed higher tensile strength and modulus, but significantly lower elongation at break. It is a fact that tensile properties of starch/flour-based materials strongly depend on their absorbed moisture content. TPFCE might be more hydrophobic than TPFC since some eugenol could be liberated from the nanoparticles by shear force during extrusion; as a result, TPFCE absorbed less water from the environment and became a stronger, stiffer, and less extensible material compared with TPFC.

Water vapor permeability (WVP) is the volume of water vapor passing through a material per unit area per unit time per unit barometric pressure, and is an important consideration when selecting a material for food packaging. TPFN exhibited WVP of 9325 g-mil/m^2-day-atm (Table 4). The value of WVP decreased to 5455 g-mil/m^2-day-atm when 0.35% (w/w) of eugenol was loaded, indicating improved water vapor barrier property of TPF. The reduction of WVP might involve the hydrophobicity of eugenol, which could migrate to the sheet surface. This result was in accordance with previous reports. The addition of essential oils, e.g. oregano, lemongrass and cinnamon, into polysaccharide matrices such as starch (Pelissari et al., 2009), chitosan (Zivanovic, Chi, & Draughon, 2005) and alginate (Rojas-Graü, Avena-Bustillos, Friedman, et al., 2006; Rojas-Graü, Avena-Bustillos, Olsen, et al., 2006) caused reduced WVP of the films due to the increased hydrophobic fraction. In addition, the incorporation of nanoparticles caused a reduction of WVP, to 5620 g-mil/m^2-day-atm for TPFC and to 4707 g-mil/m^2-day-atm for TPFCE (Table 4), indicating that the water vapor barrier property of TPF was enhanced by the incorporation of nanoparticles. This improvement might be due to two reasons: fewer free hydroxyl groups available in the TPF matrix because of H-bond formation with the nanoparticles; and a more tortuous path for water molecules to pass through (Chang et al., 2010; Ghanbarzadeh, Almasi, & Entezami, 2010). Furthermore, TPFCE exhibited lower water vapor permeability than TPFC. This might be an effect of the hydrophobicity of liberated eugenol, which corresponds to the above hypothesis.

Table 4
Water vapor permeability (WVP) and oxygen permeability (OP) of TPF sheets.

Sample	WVP* (g-mil/m^2-day-atm)	OP* (cc-mil/m^2-day-atm)
TPFN	9324.64 ± 63.16[a]	59.68 ± 2.24[c]
TPFE1	5454.55 ± 135.29[b]	59.94 ± 3.10[c]
TPFC1	5619.95 ± 199.72[b]	213.74 ± 3.06[b]
TPFCE1	4707.38 ± 83.55[c]	229.06 ± 3.34[a]

* Each value represents the mean ± SD ($n = 3$). Different superscript letters in the same column show a significant difference ($p < 0.05$) by Duncan's multiple range test.

Oxygen permeability (OP) is the volume of oxygen passing through a material per unit area per unit time per unit barometric pressure. Table 4 illustrates that TPFN and TPFE possess the same OP value of 60 cc-mil/m^2-day-atm, implying that the addition of 0.35% (w/w) of eugenol did not influence the oxygen barrier property of TPF. It should be pointed out that small molecules of hydrophobic eugenol might migrate from the TPF matrix to the sheet surface. Although oxygen molecules could solubilize in and diffuse through eugenol at the film surface, their transmission through the TPF matrix might be restricted due to the hydrophilicity and crystallinity of TPF. On the contrary, TPFC and TPFCE showed higher OP (i.e. 213.74 cc-mil/m^2-day-atm and 229.06 cc-mil/m^2-day-atm, respectively) than TPFN, indicating the diminished oxygen barrier property of TPF by incorporation of 3% (w/w) of nanoparticles. This might be explained by the decreased crystallinity of starch molecules due to obstruction by the nanoparticles. The higher OP of TPFCE compared with TPFC might be a result of the hydrophobicity of liberated eugenol. Rojas-Graü, Avena-Bustillos, Friedman, et al. (2006) and Rojas-Graü, Avena-Bustillos, Olsen, et al. (2006) revealed that the OP of apple puree edible films increased by adding essential oils, which are hydrophobic materials that can act as excellent moisture barriers but less effective gas barriers.

4. Conclusions

Thermoplastic flour (TPF) containing eugenol-loaded chitosan nanoparticles was prepared by extrusion at temperatures up to 155 °C and 170 °C to obtain products in the form of pellets and sheets, respectively. The incorporation of eugenol-loaded chitosan nanoparticles of 3–6% (w/w) did not greatly affect the crystal type and melting temperature of TPF; however it reduced decomposition temperature of TPF by about 30–35 °C. Although the addition of 3% (w/w) of eugenol-loaded chitosan nanoparticles caused decreased tensile strength (~14%), modulus (~21%) and elongation at break (~86%) of TPF, as well as increased oxygen permeability (~2.8-fold), it provided antioxidant activity and decreased water vapor permeability (~0.5-fold). In addition, TPF containing encapsulated eugenol exhibited superior radical scavenging activity (~1.3–3.3-folds) compared with TPF containing naked eugenol. The obtained TPF containing eugenol-loaded chitosan nanoparticles could potentially be applied as an antioxidant active material for food packaging.

Acknowledgments

The authors would like to acknowledge the financial support from the National Science and Technology Development Agency (NSTDA), Thailand (2009 NSTDA Chair Professor Grant funded by the Crown Property Bureau); the Research, Development and Engineering (RD&E) fund through The National Nanotechnology Center (NANOTEC), NSTDA, Thailand (Project P-11-00114) to Kasetsart University; and the Commission on Higher Education, Ministry of Education, Thailand (National Research University of Thailand). The authors are grateful to Prof. Suwabun Chirachanchai, Chulalongkorn University (Thailand), and Hitachi High-Technologies

Corp. (Japan) for morphological characterization using a TEM H-7650; and Mettler-Toledo (Thailand) for their generosity in allowing the use of TGA and DSC instruments.

Appendix A. Supplementary data

Supplementary data associated with this article can be found, in the online version, at http://dx.doi.org/10.1016/j.carbpol.2012.09.099.

References

Baskaran, Y., Periyasamy, V., & Venkatraman, A. C. (2010). Investigation of antioxidant, anti-inflammatory and DNA-protective properties of eugenol in thioacetamide-induced liver injury in rats. *Toxicology*, *268*, 204–212.

Chalier, P., Ben Arfa, A., Preziosi-Belloy, L., & Gontard, N. (2007). Carvacrol losses from soy protein coated papers as a function of drying conditions. *Journal of Applied Polymer Science*, *106*, 611–620.

Chang, P. R., Jian, R., Yu, J., & Ma, X. (2010). Fabrication and characterisation of chitosan nanoparticles/plasticised-starch composites. *Food Chemistry*, *120*, 736–740.

Choi, M. J., Soottitantawat, A., Nuchuchua, O., Min, S. G., & Ruktanonchai, U. (2009). Physical and light oxidative properties of eugenol encapsulated by molecular inclusion and emulsion–diffusion method. *Food Research International*, *42*, 148–156.

Coimbra, M., Isacchi, B., van Bloois, L., Torano, J. S., Ket, A., Wu, X., et al. (2011). Improving solubility and chemical stability of natural compounds for medicinal use by incorporation into liposomes. *International Journal of Pharmaceutics*, *416*, 433–442.

Devi, K. P., Nisha, S. A., Sakthivel, R., & Pandian, S. K. (2010). Eugenol (an essential oil of clove) acts as an antibacterial agent against *Salmonella typhi* by disrupting the cellular membrane. *Journal of Ethnopharmacology*, *130*, 107–115.

Ghanbarzadeh, B., Almasi, H., & Entezami, A. (2010). Improving the barrier and mechanical properties of corn starch-based edible films: Effect of citric acid and carboxymethyl cellulose. *Industrial Crops and Products*, *33*, 229–235.

Jayakumar, R., Prabaharan, M., Nair, S. V., Tokura, S., Tamura, H., & Selvamurugan, N. (2010). Novel carboxymethyl derivatives of chitin and chitosan materials and their biomedical applications. *Progress in Materials Science*, *55*, 675–709.

Ma, X. F., Yu, J. G., & Wan, J. J. (2006). Urea and ethanolamine as a mixed plasticizer for thermoplastic starch. *Carbohydrate Polymers*, *64*, 267–273.

Munin, A., & Edwards-Lévy, F. (2011). Encapsulation of natural polyphenolic compounds: A review. *Pharmaceutics*, *3*, 793–829.

Nam, S., Scanlon, M. G., Han, J. H., & Izydorczyk, M. S. (2007). Extrusion of pea starch containing lysozyme and determination of antimicrobial activity. *Journal of Food Science*, *72*, 477–484.

Nonsee, K., Supitchaya, C., & Thawien, W. (2011). Antimicrobial activity and the properties of edible hydroxypropyl methylcellulose based films incorporated with encapsulated clove (*Eugenia caryophyllata* Thunb.) oil. *International Food Research Journal*, *18*, 1531–1541.

Oyaizu, M. (1986). Studies on products of browning reaction: Antioxidative activities of products of browning reaction prepared from glucosamine. *Japanese Journal of Nutrition*, *44*, 307–315.

Parejo, I., Viladomat, F., Bastida, J., Rosas-Romero, A., Flerlage, N., Burillo, J., et al. (2002). Comparison between the radical scavenging activity and antioxidant activity of six distilled and nondistilled Mediterranean herbs and aromatic plants. *Journal of Agricultural and Food Chemistry*, *50*, 6882–6890.

Pelissari, F. M., Grossmann, M. V. E., Yamashita, F., & Pineda, E. A. G. (2009). Antimicrobial, mechanical, and barrier properties of cassava starch–chitosan films incorporated with oregano essential oil. *Journal of Agricultural and Food Chemistry*, *57*, 7499–7504.

Rojas-Graü, M. A., Avena-Bustillos, R. J., Friedman, M., Henika, P. R., Martín-Belloso, O., & McHugh, T. H. (2006). Mechanical, barrier, and antimicrobial properties of apple puree edible films containing plant essential oils. *Journal of Agriculture and Food Chemistry*, *54*, 9262–9267.

Rojas-Graü, M. A., Avena-Bustillos, R. J., Olsen, C., Friedman, M., Henika, P. R., Martín-Belloso, O., et al. (2006). Effects of plant essential oils and oil compounds on mechanical, barrier and antimicrobial properties of alginate–apple puree edible films. *Journal of Food Engineering*, *54*, 634–641.

Sanla-Ead, N., Jangchud, A., Chonhenchob, V., & Suppakul, P. (2012). Antimicrobial activity of cinnamaldehyde and eugenol and their activity after incorporation into cellulose-based packaging films. *Packaging Technology and Science*, *25*, 7–17.

Woranuch, S., & Yoksan, R. (2012). Eugenol-loaded chitosan nanoparticles: I. Thermal stability improvement of eugenol through encapsulation. *Carbohydrate Polymers*, http://dx.doi.org/10.1016/j.carbpol.2012.08.117

Yokesahachart, C., & Yoksan, R. (2011). Effect of amphiphilic molecules on characteristics and tensile properties of thermoplastic starch and its blends with poly(lactic acid). *Carbohydrate Polymers*, *83*, 22–31.

Zivanovic, S., Chi, S., & Draughon, A. F. (2005). Antimicrobial activity of chitosan films enriched with essential oils. *Journal of Food Science*, *70*, M45–M51.